Journal of Electron Devices, Vol. 22, 2015, pp. 1888-1894

Journal of Electron Devices
www.jeldev.org

© JED [ISSN: 1682 -3427]

[ISSN: 2412 -1150](Online)

COMPARATIVE STUDY OF CIO AND AIO TRANSPARENT CONDUCTING OXIDE THIN FILMS GROWN BY SIMPLIFIED SPRAY PYROLYSIS TECHNIQUE

P.Deepa[1, a] and P. Philominathan[2*, b]

*[1,2 *] PG and Research Department of Physics, AVVM Sri Pushpam College (Autonomous institution affiliated to Bharathidasan University, Trichy), Poondi, Thanjavur 613 503, India.*

[a]deepa13789@gmail.com, [b]philominathan@gmail.com

ABSTRACT

We wish to present a comparative report of copper doped indium (CIO) and silver doped indium oxide (AIO) thin films interms of crystallization, electrical and optical propreties as it will be a boon for the applicability in transparent conducting oxide devices. Cu doped InO and Ag doped InO thin films were deposited on glass substrates (corning 1737) using a simplified version of spray technique. XRD analysis exhibited the cubic structure and enchanced crystalline property of the films. Electrical sheet resistance of the film was found to be (20 Ω/□) Ag-doped InO thin films prepared at 450 K. Moreover, all the films exhibit good transparency for a broad wavelength range from 200 to 1200 nm and the transmittance is more than 85 % in the visible region, leading so to an increasing carrier generation towards the near infrared region of the spectrum, as required for applications such as solar cells. We also notice that increasing the doping concentration widenes the optical band gap and cause a small Burstein–Moss shift, due to mobility decrease, as expected. The SEM image of defect related to the formation of trapped states (introduction of dangling bonds) for CIO (450 K of Cu) and AIO (450 K of Ag) films.

Keywords: Perfume atomizer technique, Structural Properties, Transparent conducting oxide, CIO, AIO, Electrical properties.

I. INTRODUCTION

Transparent conducting oxide (TCO) films have been intensively investigated for optical and electrical applications, such as flat-panel displays, liquid crystal displays, organic light-emitting diodes, thin-film transistors, and thin-film solar cells [1-4]. TCO thin films should have low resistivity, high transmittance in the visible region (400 to 800 nm), and high thermal/chemical stability [5,6]. In most cases, indium tin oxide (ITO) has been widely employed as a TCO material because of its superb electrical and optical properties. However, ITO has low stability, high toxicity, high cost and is a rare material, motivating efforts to develop alternatives[7]. Indium oxide (In_2O_3) is a transparent conducting oxide which presents a high conductivity (free carrier up to 10^{17} - 10^{19} cm^{-3} range) without intentional doping [8], the origin of which is still under debate [9]. The recent trend towards higher quality and tailoring transparent conducting electrodes to constraints of specific electron and solar cell technologies demands the continuous optimisation of In_2O_3 thin film properties and processing conditions [8-9].

Thin films have been prepared by the variety of thin film deposition techniques, such as chemical vapor deposition, DC and RF magnetron sputtering, electron beam evaporation, thermal plasma, pulsed laser deposition, metal organic chemical vapor deposition, spin-coating, and sol–gel method [10-18]. To the best of our knowledge, this inexpensive spray technique using perfume atomizer may be the simplest of all deposition technique. In this present study, Cu-doped InO (hereafter CIO) and Ag-doped InO (hereafter AIO) thin films were prepared by simplified spray pyrolysis techniques since this particular technique

offers several advantages, such as large deposition area, simple equipment, low fabrication cost, and high homogeneity of the precursor. We compared this effect Cu and Ag dopants on the microstructure, electrical and optical properties of the CIO and AIO thin films as a function of various substrate temperature (300 K – 450 K).

II. EXPERIMENTAL DETAILS

Thin films were prepared by simplified spray pyrolysis technique using perfume atomizer. $Cu(CH_3COO)_2$, $InCl_3$ and $AgNO_3$ were used. The indium III chloride ($InCl_3$) was used as the source for indium, where as the copper doping was achived using copper acetate. Microscopic glass plates ($25\times25\times1.2$ mm^3) cleaned by acetone was used as substrate. Indium tricholoride was dissolved in 2 ml of concentrated HCL acid by heating it at 500° C for 10 min. The resultant transparent solution diluted with methanol forms the starting solution. $InCl_3$ was dissolved in a mixure of doubly distilled water and 10 ml of ethanol. Separately, silver nitrate was used as a dopant material which dissolved in double distilled water, finally both the solution were mixed together using magnetic stirrer. Then, the final transparent solution was manually sprayed onto preheated glass substrate. In order to study the influence of Cu and Ag dopant concentrations on the properties of Cu-doped and Ag-doped In_2O_3 thin films, with various substrate temperature 300-450 K. Hence the overall reaction process can be described as thermal decomposition of starting materials in the presence of water and air.

The prepared samples were characterized by the X-ray diffraction (XRD) patterns were obtained using the computer controlled Phillips x'pert PRO XRD system (Cukα radiation; λ=1.5405 Å) in Bragg-Brentano geometry (θ/2θ coupled). The Joint Committee on Powder Diffraction Standards (JCPDS) database from the International Centre for Diffraction Data (ICDD) was utilized for the identification of crystalline phases. The transmission data were observed in the range of 300-1100 nm using ultraviolet visible near infrared double beam spectrophotometer (Perkin Elmer). The electrical properties were studied with the use of hall effect apparatus (ECOPIA HMS-3000) with van der pauw configuration. The surface morphology was recorded by employing scanning electron microscope (HITACHI S-3000H).

III RESULT AND DISCUSSION

III.1. Structural Properties

The structural analysis of the (CIO and AIO) prepared samples was carried out by X-ray diffraction spectrometer as depicted in Figure 1a and b respectively. Well defined peak at 22° corresponding to reflection (2 1 1) plane was observed in 300 K. This indicates that all samples are polycrystalline and matched the characteristic peaks of the cubic In_2O_3 phases (JCPDS 00-006-0416). The strong diffraction peaks of the films changed from the (2 1 1) to plane to the (2 2 2) plane. If the respective ion, the change in the preferred orientation may not occurs. However, if the

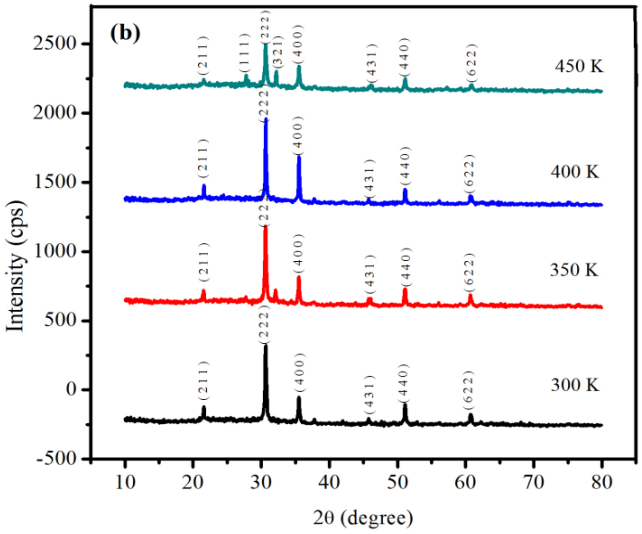

dopant occupies additional interstitial sites which are

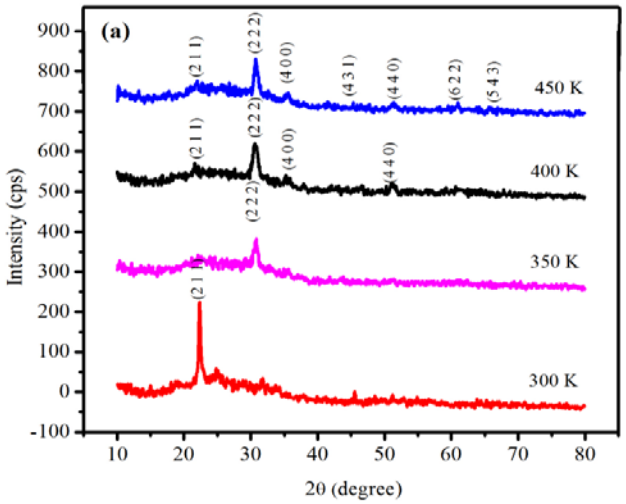

unoccupied, a change in the preferred growth take place. The Mo incorporated at additional interstitial sites changes the preferred orientation of the films. The change in preferential orientation was also observed in Sn doped In_2O_3 films by Agashe and Mahamuni [19]. Moreover, for all the samples, no peaks corresponding to CuO phase could be detected. It is also seen that the intensity of the peaks gradually decreases as the deposition temperature increased, showing the degradation of crystalline quality which may be attributed to the compression stress arising from the different ionic radii of substituted Cu^{2+} (7.3×10^{-11} m) on In^{2+} (8.1×10^{-11} m) [20]. Fig. 1b shows that the prepared

films show six well defined diffraction peaks along with low intensity peak corresponding to In_2O_3 phase with cubic structure (JCPDS No. 00-006-0416). The intensity of the diffraction peaks was slightly increased, thereafter it got decreased when the substrate temperature approached 450 K as evident from Fig. 1b, the samples prepared at high substrate temperature additionally two diffraction peaks (1 1 1) and (3 2 1) was found which corresponding to In_2O_3 phase. The diffraction peaks of AIO films are sharp and it shows increase in the intensity of preferred orientation compare to CIO films, the reason of CIO films are less crystalline due to defects and lack of enough kinetic energy and mobility of the grains to get oriented at respective planes. Defects/ imperfections/ oxygen vacancies of the crystal lattice decrease on CIO films. AIO films enhance thermal energy and mobility of the grains by increasing intensity of preferred orientation and stoichiometry of the films [21]. The average crystalline size was estimated by using the well-know scherrer's formula [22], The result imply that the grain size of CIO and AIO thin films size increases with increasing substrate temperature, the obtained crystallite size was found to be in the nano range (20 nm(CIO), 31 nm(AIO)) films, and it is observed that the grain size of AIO films is larger than that of CIO films. The foregoing discussions lead to the comparison of CIO and AIO films, the diffraction peaks of AIO films are sharp and it shows better crystalline behavior than CIO films, which may be due to two possible reasons: (i) the increasing number of nucleation leading to the formation of small grains during incorporation of

Figure 1: XRD scans with Cu-Kα radiation for thin films at different Cu and Ag concentrations. (a) CIO and (b) AIO thin films.

the dopant into the host material and (ii) the disturbance of grain growth by stress due to the difference in ionic radius between Cu and indium [23]. However, when viewing the case of CIO, the second reason seems more suited since the grain size of the CIO thin films.

The variation in crystallite size can be explained on the basis of the Zener pinning effect [24]. When Ag doped with In ions AIO (450 K of Ag) may fill the oxygen vacancies, and consequently the zener pinning effect is suppressed resulting in the growth of larger crystallites. However, CIO (450 K of Cu) the Zener pinning effect again comes into play, but due to the interstitial incorporation of Cu, in this instance. The result imply that the grain size of CIO(12, 15, 18, 20) and AIO(14, 19, 24, 31) thin films size increases with increasing substrate temperature, the grain size of AIO films is larger than that of CIO films. This result supports the observation on the AIO (450 K of Ag) induced improvement in the crystallinity of the films. This increase in cryatallinite size is a consequence of the coalescence of crystallites caused by the sufficient

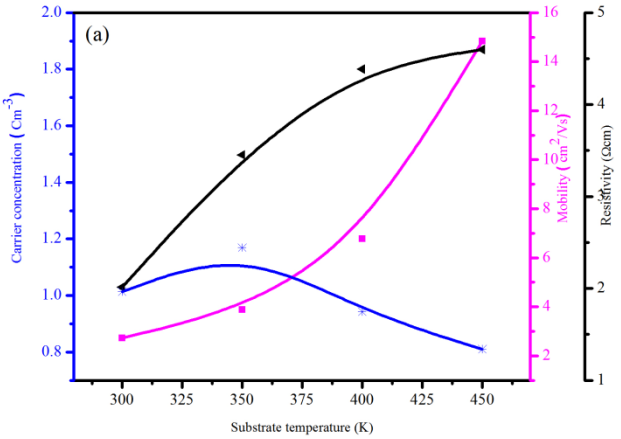

thermal energy supplied during the Ag doped Indium oxide film deposited at 450 K.

III.2. Electrical properties

The Hall measurements were performed at room temperature in van der pauw configuration. The negative sign of Hall co-efficient confirmed n-type conductivity. Fig. 2(a,b) summarizes electrical resistivity results of CIO and AIO thin films.

Sample	Substrate temperature (°C)	Resistivity $\rho\times10^{2}$ (Ωcm)	Mobility μ(cm^2 v^{-1}s^{-1})	Carrier concentration ($n\times10^{20}$cm^{-3}) and type of charge carrier	Sheet resistance R(Ω/□)	Figure of merit $F_{TC}\times10^{3}\Omega^{-1}$	Transmission T(%)
CIO	300K	4.61	4.8	-0.85	515	0.3	68%
CIO	350K	6.41	10.2	-0.95	175	2.4	75%
CIO	400K	3.8	13.7	-1.2	90.0	5.8	86%
CIO	450K	2.27	14.5	-1.9	83.0	7.9	94%
AIO	300K	6.19	15	-1.22	79.0	5.9	69%
AIO	350K	3.14	19	-9.28	62.0	6.5	80%
AIO	400K	1.23	99	-5.07	34.0	7.2	90%
AIO	450K	1.29	73	-6.55	20.0	8.7	97%

Table 1: Some typical parameters of sprayed CIO and AIO thin films.

The values of carrier density obtained are -1.9×10^{20} and -6.55×10^{20} cm^{-3} for CIO (450 K of Cu) and AIO (450 K of Ag) respectively. The difference can be attributed to substantial disordered states with dopant atoms not activated between crystalline grains, when taking the electrical measurements, which lead to an increase of the electrical resistivity. We obtain $\rho = 2.27\times10^{-2}$ Ωcm and $\rho=1.29\times10^{-2}$ Ωcm as electrical resistivity for CIO (450 K of Cu) and AIO (450 K of Ag) respectively. From Table 1, the electrical resistivity values of our samples are same order magnitude in the literature. They correspond to degenerate semiconductors with high free-electron concentration, more than 10^{20} cm^{-3}. In CIO with cubic structure, it is due to contribution of

substitutional Cu and to oxygen vacancies (negative donors). Similarly, Ag^{-} substitutes O^{2-} in the indium oxide lattice for AIO films. For this substitution, the electrical perturbation is largely confined to the filled valence band and the scattering of electrons is reduced leading to a decrease of resistivity. The values of mobility are small by less than one order of magnitude of the best published values [25,26] because of the ionized scattering centers. The degeneracy of our samples is confirmed by the evaluation of the Fermi energy level using the relation [27]:

$$E_f = \left(\frac{h^2}{8m^*}\right)\left(\frac{3n}{\pi}\right)^{2/3} \quad (1)$$

where m* is the value of effective mass, $0.19m_e$ (m_e is the rest mass of electron) and n is the carrier concentration. The calculated E_F values are 1.43 eV for CIO and 0.89 eV for AIO respectively, which are higher than the energy
corresponding to the room temperature. In the case of a transparent conducting oxide film, both the optical transmission and electrical conductivity should be as large as possible for applications in optoelectronic devices. A way for evaluating this is by means of the figure of merit and it is given by $\Phi_{TC} = T/ R_S$, where R_S is the sheet

Figure 2: **R**esistivity, hall mobility, and carrier concentration of (a) CIO and (b) AIO thin films.

resistance given in Table 1, and T is the optical transmittance [28]. Considering the application of the films to display devices, we have chosen to determine the average transmittance by using the equation .

$$T_{av} = \frac{\int V(\lambda)T(\lambda)d\lambda}{\int V(\lambda)d\lambda} \quad (2)$$

where T(λ) is the transmittance and V(λ) is the photopic luminous efficiency function defining the standard observer for photometry [29]. Although the figure of merit obtained by using this transmittance value might be lesser than that obtained using the peak value of transmittance, or the linearly averaged value of transmission as is usually done, this approach gives a more realistic estimate of the actual merit of the film for display device applications as the photopic function is a measure of the sensitivity of the human eye. The figure of merit obtained 7.9×10^{-3} Ω^{-1} and 8.7×10^{-3} Ω^{-1} for CIO and AIO respectively, with best figure of merit value obtained AIO film in a good agreement with earlier work [30]. These F_{TC} results indicate the promise of these films to potential applications in transparent conducting electrode like solar cells and as a work electrode in electrodeposition process [31].

III.3. Optical properties

The optical transmittance spectra of the CIO and AIO films are shown in Figure 3a,b respectively. The transmittance in the visible range lies between 85 % and 87 % which is ideal for window layers in solar cells [32]. The oscillatory behavior of the transmission curve is caused by the interference phenomenon indicating the uniformity of the coatings. The high optical transmittance of the films is generally due to the high mobility of charge carriers, ability of the roughness of the films surface to reduce reflectivity, an increase in the structured homogeneity, a decrease in the diffuse scattering and fine texturing [33]. In the present work, the X-ray diffraction studies strongly supported the fine texturing of the films. The transparency window of the films is wide enough, so that it can be considered as a typical TCO suitable for solar cell applications. E_g of the samples is estimated from the optical bandgap can be obtained by

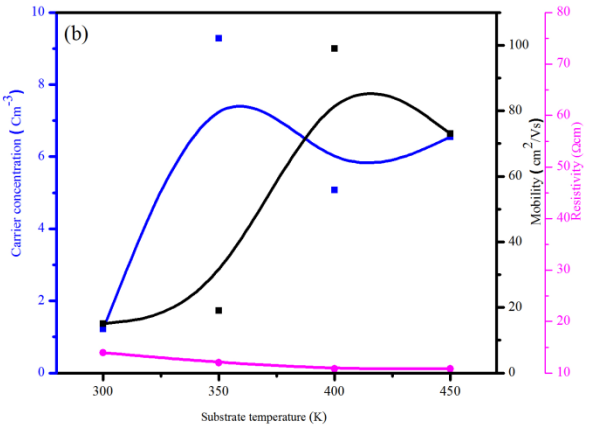

extrapolating the corresponding straight lines downwards to the photon energy axis in Tauc's plot drawn for $(\alpha h\upsilon)^2$ against photon energy ($h\upsilon$). The optical bandgap increased in accordance with an increase in the Cu and Ag doping concentrations.

The value of CIO thin films is about from 2.1 to 2.5 eV and for AIO thin films is from approximately 2.3 to 2.6 eV. According to the Burstein-Moss effect, the broadening of the optical bandgap is given as follows:

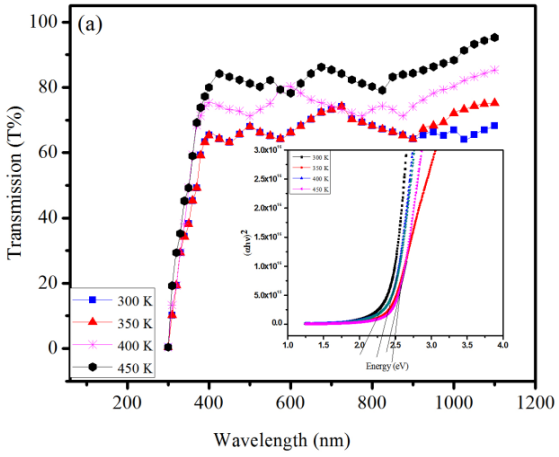

$$\Delta E_g = \left(\frac{h^2}{2m^*_{vc}}\right)(3\pi^2 n)^{2/3} \qquad (3)$$

Where ΔE_g is the shift of the doped semiconductor compared to undoped semiconductor, m^*_{vc} is the reduced effective mass, h is Plank's constant, and n is the carrier concentration. According to this equation, the optical bandgap would increases with increasing carrier concentration.

III.4. Morphological properties

The microstructure of CIO and AIO thin films have an influence on the electrical and optical properties for optoelectronic devices, it is very important to investigate the surface morphology of CIO and AIO thin films. Fig. 4 shows the SEM image of CIO (Fig. 4a) and AIO (Fig. 4b) thin films with different substrate temperature (300, 350, 400 and 450 K) respectively. In the case of CIO and AIO films(Fig. 4a, 4b) spherical shaped grains and exhibits good surface homogeneity. This surface homogeneity is also one of the reason for the obtained interference pattern in the transmittance spectra. Upon increase in substrate temperature (CIO and AIO film) along with the change in the shape of the grains was observed. This could provide the larger surface to volume ratio and yield the formation of large number of dangling bonds. The existence of dangling bonds in a crystal surface leads to the formation of localized states related to the structural defects within the band gap [34]. In the present study is confimed by the XRD profiles of CIO and AIO thin films as evident from Fig. 1 (section 3.1).

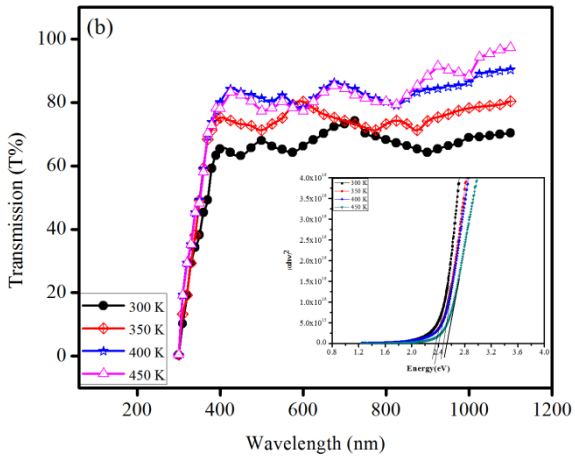

Figure 3: Variation of transmittance (T%) with wavelength λ (nm) of ((a) CIO (b) AIO) thin films. Inset shows the (hυ) vs $(\alpha h\upsilon)^2$ curve extrapolated to obtain the optical band gap.

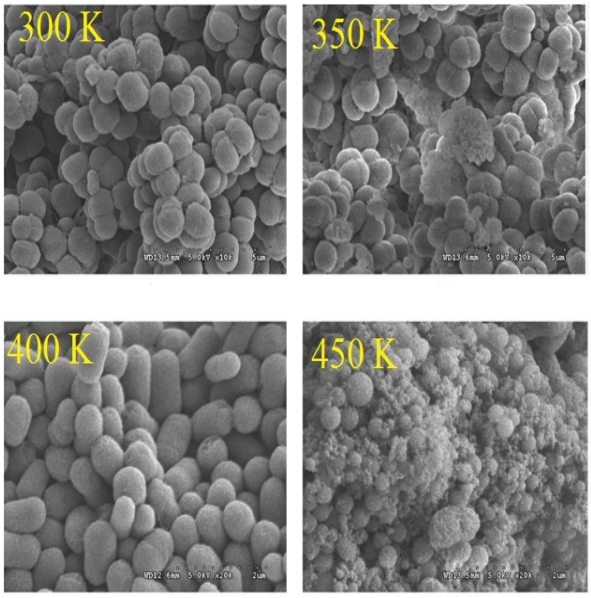

Figure 4a: SEM image of CIO thin film as a function of different substrate temperature.

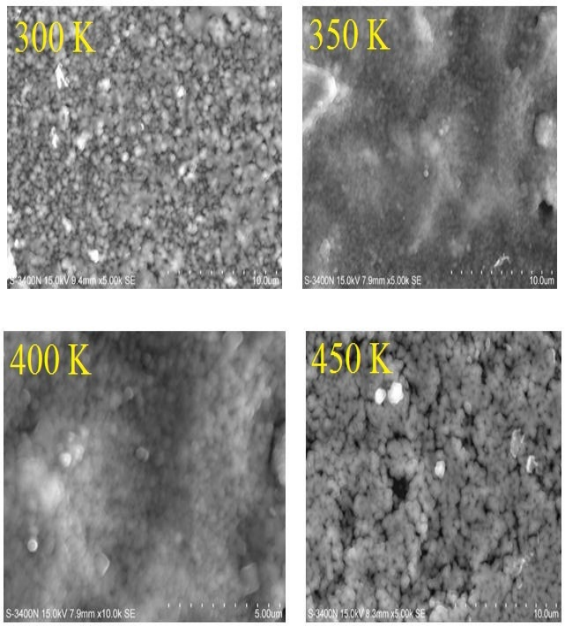

Figure 4b: SEM image of AIO thin film as a function of different substrate temperature.

IV CONCLUSION

The low-cost and very much simplified spray technique using perfume atomizer has been employed to fabricate (CIO and AIO) films with good structural, electrical optical and morphological properties. All films had a cubic crystal structure, and a minimum sheet resistance of 20 Ω/□,high carrier mobility (73 cm^2/Vs), a low resistivity ($1.29\times10^{-2}\Omega$ cm) and carrier concentration (1.9×10^{20} cm^{-3}) were achieved for the film deposited at AIO (450 K of Ag) thin film. F_{TC} results 7.9×10^{-3} Ω^{-1} and 8.7×10^{-3} Ω^{-1} for CIO and AIO indicate the promise of these films to potential applications in transparent conducting electrode like solar cells. The transmittance of the CIO and AIO thin films were higher than 85 % in the visible region, and the optical bandgap of the CIO and AIO thin films became broader with increasing Cu or Ag deposition temperature because of the Burstein-Moss effect. The SEM images of the film exhibits good surface homogeneity. In concluded, the structural, electrical, optical and morphological characteristics of CIO and AIO thin films were observed, and Cu doping seems to be more effective than Ag doping. The films were found to have good physical properties desirable for solar cell applications.

References

1. M. Ohyama , H. Kozuka and T. Yoko, “Sol–gel preparation of transparent and conductive aluminum-doped zinc oxide films with highly preferential crystal orientation”, J Am Ceram Soc. 81, 1622 (1998).

2. K.Y. Cheong, N. Muti and S.R. Ramanan, “Electrical and optical studies of ZnO:Ga thin films fabricated via the sol–gel technique”, Thin Solid Films. 10, 142 (2002).

3. J.H. Lan, J. Kanicki, A. Catalano, J. Keane, W.D. Boer and T.J. Gu, “Patterning of transparent conducting oxide thin films by wet etching for a – Si:H TFT-LCDs”, Electron Mater. 25, 1806 (1996).

4. B. Rech and H. Wagner, “Potential of amorphous silicon for solar cells”, Appl. Phys. A. Mater Sci Process. 69, 155 (1999)s.

5. G. Gordillo and C. Calderon, “Properties of ZnO thin films prepared by reactive evaporation”, Solar Energy Mater. Solar Cell. 69, 251(2001).

6. M. Oztas and M. Bedir, “Thickness dependence of structural, electrical and optical properties of sprayed ZnO:Cu films”, Thin Solid Films. 516, 1703 (2008).

7. M. Chen, Z.L. Pei, C. Sun, J. Gong, R.F. Huang and L.S. Wen, “ZAO: an attractive potential substitute for ITO in flat display panels”, Mater Sci and Eng B. 85, 212 (2001).

8. A. Facchetti and T.J. Marks (Eds.), “Transparent Electronics From Synthesis to Applications”, John Wiley & Sons Ltd., United Kingdom. (2010).

9. S. David, Ginley, Hideo Hosono and C. David, Paine (Eds.), Handbook of Transparent Conductors, Springer, New York Heidelberg Dordrecht London. (2011).

10. J. Nishino, T. Kawarada, S. Ohshio, H. Saitoh, K. Maruyama and K. Kamata, “Conductive indium-doped zinc oxide films prepared by atmospheric pressure chemical vapour deposition”, J Mater Sci Lett. 16, 629 (1997).

11. N.F. Cooray, K. Kushiya , A. Fujimaki, I. Sugiyama, T. Miura, D. Okumura, M. Sato, M. Ooshita, and O. Yamase, “Large area ZnO films optimized for graded bandgap Cu(InGa) Se2-based thin-film mini-modules”, Sol Energy Mater and Sol Cells. 49, 291(1997).

12. O. Kluth, G. Schope, B. Rech, R. Menner, M. Oertel, K. Orgassa and H.W. Schock, “Comparative material study on rf and dc magnetron sputtered ZnO:Al films”, Thin Solid Films. 502, 311(2006).

13. A. Kuroyanagi, “Properties of aluminum-doped ZnO thin films grown by electron beam evaporation”. Jpn J Appl Phys. 28, 219 (1989).

14. R. Groenen, J.L. Linden, H.R.M. van Lierop, D.C. Schram, A.D. Kuypers and M.C.M. van de Sanden, “An expanding thermal plasma for deposition of surface textured ZnO:Al with focus on thin film solar cell applications”, Appl Surf Sci. 173, 40 (2001).

15. E.S. Sub, H.S. Kang, J.S. Kang, J.H. Kim and S.Y. Lee, “Effect of the variation of film thickness on the structural and optical properties of ZnO thin films deposited on sapphire substrate using PLD”, Appl Surf Sci. 186, 474 (2002).

16. Z. Fu , B. Lin and J. Zu , "Photoluminescence and structure of ZnO films deposited on Si substrates by metal-organic chemical vapor deposition", Thin Solid Films. 402, 302 (2002).
17. P. Nunes, B. Fernandes, E. Fortunato, P. Vilarinho and R. Martins, "Performances presented by zinc oxide thin films deposited by spray pyrolysis", Thin Solid Films. 337, 176 (1999).
18. W. Tang and D.C. Cameron, "Aluminum-doped zinc oxide transparent conductors deposited by the sol–gel process", Thin Solid Films. 238, 83(1994).
19. C. Agashe and S. Mahamuni, "Doping-induced changes in the physical properties of In_2O_3:Sn films", Semicond. Sci. Technol. 10, 172-178 (1995).
20. D. Beena, R. Vinodkumar, I. Navas, V. Ganasen, A. Yamuna and V.P. Mahadevan Pillai, "Transparent conducting indium molybdenum oxide films by pulsed laser ablation", Journal of Alloys and Compounds. 539, 63-68 (2012).
21. D. Beena, K.J. Lethy, R. Vinodkumar, A.P. Detty, V.P. Mahadevan Pillai and V. Ganesan, "Photoluminescence in laser ablated nanostructured indium oxide thin films", Opto electronics and advanced materials. 5(1), 1-11 (2011).
22. Buerger Azaroff, Powder method in X-rey crystallography, (1958).
23. Hu J and Gordon RG, "Textured aluminum-doped zinc oxide thin films from atmospheric pressure chemical- vapor deposition", J Appl Phys. 72, 5381(1992).
24. N. Moelans, B. Blanpain, P. Wollants, "Pinning effect of second-phase particles on grain growth in polycrystalline films studied by 3-D phase field simulations", Acta Materialia. 55, 2173-2182 (2007).
25. J.H. Kim, K.A. Jeon, G.H. Kim and S.Y. Lee, "Electrical, structural, and optical properties of ITO thin films prepared at room temperature by pulsed laser deposition", Appl. Surf. Sci. 252, 4834 (2006).
26. T. Fukano and T. Motohiro, "Low-temperature growth of highly crystallized transparent conductive fluorine-doped tin oxide films by intermittent spray pyrolysis deposition", Sol.Energy Mater. Sol. Cells. 82, 576 (2006).
27. B. Thangaraju, "Structural and electrical studies on highly conducting spray deposited fluorine and antimony doped SnO2 thin films from SnCl2 precursor", Thin Solid Films. 402, 71 (2002).
28. H.L. Hartnagel, A.L. Dawar, A.K. Jain and C. jagadish, "Semiconducting Transparent Thin Films (Bristol: Institute of Physics Publishing)" 306 (1995).
29. W.G. Driscoll and W. Vaughan, Handbook of Optics (McGraw-Hill, USA, 1978).
30. K. Sivaramakrishnan and T.L. Alford, "Metallic conductivity and the role of copper in ZnO/Cu/ZnO thin films for flexible electronic", Applied Physics Letter. 94, 052104 (1995).
31. M. Ait Aouaj, M. Abd-lefdil, F. Cherkaoui, E.I. Moursli and F. Hajji, "Ag/ITO transparent conducting oxides", Eur. Phys. J. Appl. Phy. 40, 55 (2007).
32. R.R Biswal, S. Valumani, B.J. Babu, A. Maldonado, S. Tirado-Guerra, L. Castaneda, M. de la and L. Olvera, "Fluorine doped zinc oxide thin films deposited by chemical spray, starting from zinc pentanedionate and hydrofluoric acid: Effect of the aging time of the solution", Master. Sci. Eng. B. 174, 46-49 (2010).
33. K. Ramamurthy, C. Sanjeeviraja, M. Jayachandran, K. Sankaranarayanan, P. Misra and L.M. Kukreja, "Development of a novel high optical quality ZnO thin films by PLD for III-V opto-electronic devices", Curr. Appl. Phy. 6, 103-108 (2006).
34. Xiaofang, Wang, Fuli. Zhao, Pingbo. Xie, Shaozhi. Deng, Xu. Ningsheng, Hezhou Wang, "Surface emission characteristics of ZnO nanoparticles", Chem. Phys. Lett. 423, 361-365 (2006).
35. A. M. Suhail, S. Salman, F. E. Naoum, H. A. Thjeela, and Q. G. Al zaidia, "ZnO/Porou silicon photovoltaic UV detector", Journal of Electron Devices. 13, 900-909 (2012).
36. Aniruddh Bahadur Yadav, Amritanshu Pandey and S. Jit, Pd Schottky, "Contacts on Sol-Gel Derived ZnO Thin Films with Nearly Ideal Richardson Constant", IEEE Electron Device Letters, 35, 729-730 (2014).